EFFECT OF OXIDATION STATES ON THE SYNGAS ACTIVITY OF TRANSITION-METAL OXIDE CATALYSTS

By

J. R. Monnier and G. Apai

Research Laboratories, Eastman Kodak Company,
Rochester, New York 14650

INTRODUCTION

Supported Rh catalysts and Rh-containing mixed oxide catalysts have been studied extensively (1-5) for Fischer-Tropsch activity and their ability to produce different distributions of oxygenated products. Ichikawa and co-workers (1, 2) correlated X-ray photoelectron spectroscopy (XPS) measurements on the electronic state(s) of supported Rh catalysts with their corresponding Fischer-Tropsch oxygenate distributions and concluded that for selective C_2-oxygenate formation both Rh^0 and Rh^+ sites were required; the Rh^0 sites functioned as CO dissociation sites in the formation of alkyl groups, while Rh^+ served as the site for associative CO adsorption and subsequent CO insertion to form intermediate acyl species. Similarly, Wilson et al. (3) concluded that the stabilization of Rh^+ by Mn promoters in silica-supported Rh catalysts may be responsible for the enhanced C_2-oxygenated selectivity under syngas reaction conditions.

Somorjai and co-workers (4, 5), using a different approach, studied the syngas activity of Rh_2O_3 and $LaRhO_3$ at different temperatures and presumably different levels of reduction and also concluded that for selective C_2 and C_2^+ oxygenate formation to occur efficiently, Rh^0 and Rh^+ are required for facile CO dissociation and CO insertion, respectively. Thus there are strong implications as to the importance of oxidation states of group 8 metals in controlling the linear oxygenate selectivity and product distribution. To better understand the relationship between transition-metal oxidation states and catalytic

performance, we synthesized high-purity $LaRhO_3$ and $GdCoO_3$ and characterized and evaluated these catalysts at different levels of reduction to determine the existence and thus the importance of different Rh and Co oxidation states. Where appropriate, comparisons are made with a conventional Rh/SiO_2 catalyst.

Cu-based, low-pressure CH_3OH synthesis catalysts represent another system in which oxidation states are important. Recent evidence suggests that Cu^+ species are the active components for CO activation in both Cu-ZnO (6) and Cu-Cr oxide (7, 8) catalysts. Others (9), however, have used XPS to examine the oxidation states of Cu in Cu-ZnO and report the existence of only Cu^0 species under reaction-like reducing conditions. Yet others (10) propose that both Cu^0 and Cu^+ are essential for selective CH_3OH formation, with Cu^+ providing sites for CO activation and Cu^0 the sites for dissociative H_2 chemisorption. We present data for alkali- and alkaline-earth-promoted Cu-Cr oxide that support the hypothesis that Cu^0 serves as the site for H_2 chemisorption and that both Cu^0 and Cu^+ sites are required for Cu-Cr oxide to efficiently catalyze the formation of CH_3OH from syngas.

RESULTS AND DISCUSSION

Characterization and Catalytic Activity of $LaRhO_3$ and $GdCoO_3$

We prepared $GdCoO_3$ by high-temperature calcination (650 °C) of the stoichiometric thermal precursor $GdCo(CN)_6 \cdot nH_2O$, using the method outlined by Gallagher (11). We prepared $LaRhO_3$ in high purity by converting a mixture of La_2O_3 and Rh_2O_3 (5% excess of La_2O_3 over the 1:1 stoichiometry) to the nitrates, using HNO_3, and then firing in air to 1000 °C for 24 h. The excess La_2O_3 was removed from $LaRhO_3$ by leaching with warm 20% acetic acid (12-14). Powder X-ray diffraction

measurements showed that both $GdCoO_3$ and $LaRhO_3$ were of high purity; no diffraction lines that could be attributed to the simple oxides were detected in either sample.

The temperature-programmed reduction (TPR) spectra of $LaRhO_3$ and $GdCoO_3$ (Figure 1) illustrate their stability with respect to reduction in flowing H_2 at 1 atm pressure. Under reaction conditions used in this study, 800 psig of $H_2/CO = 1/1$, the TPR peaks would be shifted to lower temperatures. We calculated the extent of the shift for the H_2O peaks of the $GdCoO_3$ sample, using the method described by Gentry et al. (15). Under reaction conditions, the H_2O peaks centered at 415 and 515 °C would be shifted to ~307 and 390 °C, respectively. A shift of about 100 °C under reaction conditions should be expected for $LaRhO_3$ too, giving an H_2O peak centered at ~300 °C.

Prior to catalytic evaluation, $GdCoO_3$ was subjected to various levels of prereduction by stopping the TPR experiment at different temperatures. The levels of reduction were determined from the number of H_2O molecules formed during reduction. These data are summarized in Table I; the sample corresponding to 30% reduction was prepared in a recirculation loop reactor maintained at 510 °C. Table I also gives the relevant reduction data for $LaRhO_3$. Powder X-ray diffraction (XRD) measurements for the $GdCoO_3$ samples reduced to the 20% and 30% levels showed peaks for Co^0 and Gd_2O_3 only. The XRD pattern for the 10% reduced sample gave peaks corresponding to Gd_2O_3 (and by necessity Co^0, since any cobalt oxide formed along with Gd_2O_3 would be reduced to Co^0), $GdCoO_3$, and a phase tentatively identified as the defect-type perovskite, $GdCo_{0.92}O_{2.5}$.

The powder XRD of the $LaRhO_3$ sample after the TPR experiment gave only broad peaks for Rh^0 and La_2O_3. This is important, since the TPR conditions are similar to those encountered under Fischer-Tropsch

reaction conditions. X-ray photoelectron spectra of $LaRhO_3$ after various in situ reduction pretreatments (Figure 2) show that only Rh^0

Table I. Temperature-Programmed Reduction Data for $GdCoO_3$ and $LaRhO_3$

	T_{max} (° C)	#O^{2-} removed	% reduction[a]
$GdCoO_3$[b]			
	510	7.1×10^{24}	30
	535	4.6×10^{20}	20
	490	3.0×10^{20}	13
	455	2.2×10^{20}	10
$LaRhO_3$[c]			
	535	1.45×10^{20}	24

[a]Maximum extent of reduction under these conditions is 50%, since both Gd_2O_3 and La_2O_3 are stable with respect to reduction at T <800 °C. [b]350-mg sample contains 2.4×10^{21} O^{2-}. [c]100-mg sample contains 6.1×10^{20} O^{2-}.

is present on the surface after H_2 (1 atm pressure) reduction at 300 °C. Reduction at 300 °C in a 2:1 H_2/CO flow at 1 atm total pressure, however, stabilizes some of the $LaRhO_3$ from reduction to Rh^0, as evidenced by the Rh^{3+} peak. Deconvolution of the Rh $3d_{5/2}$ portion of the XPS spectrum could be fitted into two Gaussian components attributable to Rh^{3+} and Rh^0, with no Rh^+ component in the 308-eV region of the spectrum. These results differ from those of Somorjai under similar conditions, which may be due to the difference in purity of the starting $LaRhO_3$ samples. Repetition of the preparative technique outlined by Somorjai resulted in a residual Rh_2O_3 component

as detected by XPS, which was readily reduced to Rh^0 after H_2 reduction at 250 °C.

The Fischer-Tropsch activities for $LaRhO_3$ at different reaction temperatures are displayed as Schulz-Flory plots in Figure 3. At reaction temperatures ≥300 °C, the rates of C_2-oxygenates (CH_3CHO + C_2H_5OH) are greater than for CH_3OH, suggesting that the mechanism for CH_3OH formation is different from the mechanism for formation of higher oxygenates; the latter products apparently formed by CO insertion into surface alkyl fragments, as others (1, 16) have noted. Since XPS did not detect any Rh^+ on $LaRhO_3$ after a much milder pretreatment at 300 °C and the TPR curve showed that at 400 °C in 1 atm of H_2, 50% of the lattice O^{2-} associated with Rh in $LaRhO_3$ had been removed, it is difficult to envision the existence of stable Rh^+ on the catalyst surface under our reaction conditions.

The Fischer-Tropsch results for reduced $GdCoO_3$ (Figure 4) corroborate those for $LaRhO_3$ and show that the most highly reduced samples form the highest proportion of C_2 and greater oxygenates. Again, it is difficult to envision the existence of partially oxidized, catalytically active Co species after those high levels of catalyst reduction.

These results suggest there is no need to invoke Rh^+ or lower-valent oxidation states of Co to explain the higher rates of C_2-oxygenate formation. Rather, the poor CO dissociation capabilities of Rh^0 and Co^0 (17) require high temperatures and/or large metallic aggregates to efficiently dissociate CO and form surface alkyl fragments in high enough surface concentration, so that CO insertion into the metal-alkyl bond (to form acyl species) can compete favorably with hydrogenation of adsorbed CO and surface alkyls to form CH_3OH and paraffins, respectively.

This conclusion is supported by the results from a TPD/TPR sequence for CO adsorbed on a conventional 1.5% Rh/SiO_2 catalyst. The Fischer-Tropsch activity at 270 °C, 850 psig, and 2:1 H_2/CO gave 25% molar oxygenate selectivity and a C_2-oxygenate/CH_3OH ratio of 2.5. The TPD analysis in flowing He gave multiple CO desorption peaks with T_{max} values ranging from 70 to 257 °C, as well as a large CO_2 peak (from disproportionation of CO) centered at 300 °C. The TPR analysis in flowing H_2 immediately after the TPD experiment (no additional catalyst treatment) gave a large CH_4 peak centered at 219 °C. This series of experiments shows that high temperatures are required for CO dissociation to occur efficiently on supported Rh^0 surfaces and that hydrogenation of the surface carbon to form CH_4 (or surface alkyls) occurs easily once the C-O bond is ruptured. The presence of CO desorption peaks at temperatures up to 257 °C also shows that associatively adsorbed CO is present under typical reaction conditions.

Characterization and Catalytic Activity of Promoted Cu-Cr Oxide

In earlier studies (7, 8), we showed that specific rates of CH_3OH formation were proportional to the amount of $CuCrO_2$ in the Cu-Cr oxide catalyst and the fraction of Cu^+ present on the surface of the catalyst, which also contained Cu^0. One may thus expect that high-purity $CuCrO_2$, which is stable under reaction conditions, would be most active. The data in Table II show that this is not the case and suggest that Cu^0 is essential for the reduction of CO to form CH_3OH.

A series of alkali- and alkaline-earth-promoted Cu-Cr oxides (at the same molar loading) were prepared from the same batch of Cu-Cr oxide and evaluated for CH_3OH formation. The results and relevant kinetic information (Table III) show a strong promotional effect for

Table II. Effect of High-Temperature Calcination on Catalytic and Physical Properties of Cu-Cr Oxide

catalyst	surface area (m^2/g)	activity $\left(\frac{\mu mol\ CH_3OH}{s\text{-}m^2\ catalyst}\right)$	$\left(\frac{Cu^+}{Cu_{tot}}\right)$[a]	composition[b] after T_{red} = 270 °C in H_2
1/1 Cu/Cr (T_{calc} = 350 °C, for 2 h)	21.4	0.02	0.21	$CuCrO_2$ (minor) Cu^0 (major)
1/1 Cu/Cr (T_{calc} = 1000 °C, for 4 h)	2.9	0.06	0.5	$CuCrO_2$ (major) Cu^0 (major)
1/1 Cu/Cr (T_{calc} = 1000 °C, for 24 h)	0.3	≈0	1.0	$CuCrO_2$ (only)

[a]Determined by XPS after H_2 reduction at 270 °C. [b]Determined by powder X-ray diffraction.

CH_3OH formation and a lowering of the apparent activation energy for CH_3OH formation when a promoter is present.

The H_2 and CO chemisorption data in Table IV show that the enhanced catalytic activity is not due to an increase in CO adsorption (Cu^+ sites). The TPD spectra of CO for unpromoted, Ba-promoted, and Cs-promoted Cu-Cr oxides are virtually identical in normalized intensities and position (T_{max}), supporting the conclusion that CO activation is not the source of the promoter effect; likewise, XPS measurements gave essentially identical surface fractions of Cu^+ for these samples.

Table III. Rates of CH_3OH Formation and Kinetic Parameters for Promoted Cu-Cr Oxide Catalysts. Reaction Conditions: 270 °C, H_2/CO = 2/1, 800 psig pressure

catalyst	surface area (m^2/g)	rate $\left(\frac{\mu mol}{g\ cat\text{-}s}\right)$	rate $\left(\frac{\mu mol}{m^2\ cat\text{-}s}\right)$	E_{app} $\left(\frac{kcal}{mol}\right)$	reaction orders (H_2)	reaction orders (CO)
Cu-Cr oxide	69.2	0.61	0.009	19.4	0.56	0.57
(3.4% K) Cu-Cr oxide	--	9.30	--	--	--	--
(11.2% Cs) Cu-Cr oxide	75.0	9.83	0.13	13.4	--	--
(3.5% Ca) Cu-Cr oxide	--	3.74	--	--	--	--
(7.7% Sr) Cu-Cr oxide	--	9.04	--	--	--	--
(12% Ba) Cu-Cr oxide	56.8	14.54	0.26	10.9	0.56	0.62

The H_2 chemisorption data show that although the H_2 chemisorption values at the reaction temperature of 250 °C vary only slightly, the temperature dependencies for H_2 chemisorption are much lower for the promoted catalysts. This lower temperature dependency for H_2 chemisorption may be reflected in the lower E_{app} values for CH_3OH formation. The sites for H_2 chemisorption appear to be Cu^0 centers, since there was no measurable H_2 uptake on ultrapure $CuCrO_2$ (no surface Cu^0 detected by XPS) or Cr_2O_3 at 250 °C, yet H_2 chemisorption readily occurred at 250 °C on 99.99% Cu^0 powder (Aldrich).

In addition, the levels of reduction of both the Ba- and Cs-promoted samples were ~1/3 that of the unpromoted sample, 12% vs. 37%, respectively, as determined by quantitative TPR and neutron activation analysis. Therefore, the comparable levels of H_2 chemisorption at 250 °C imply greater Cu^0 particle dispersions for the promoted samples.

Table IV. H_2 and CO Chemisorption Data for Ba-Promoted, Cs-Promoted, and Unpromoted Cu-Cr Oxides

catalyst	(molecules/m² catalyst) T = 25 °C	T = 150 °C	T = 250 °C
Cu-Cr oxide (69.2 m²/g)			
H_2	1.8×10^{16}	1.4×10^{17}	6.2×10^{17}
CO	6.0×10^{16}	--	3.2×10^{17}
(Ba) Cu-Cr oxide (56.8 m²/g)			
H_2	1.4×10^{17}	3.9×10^{17}	6.2×10^{17}
CO	8.6×10^{16}	--	5.1×10^{17}
(Cs) Cu-Cr oxide (75 m²/g)			
H_2	1.3×10^{17}	2.1×10^{17}	2.6×10^{17}
CO	1.2×10^{17}	--	6.2×10^{17}

This observation is corroborated by the XRD patterns (Figure 5) of unpromoted and Ba-promoted Cu-Cr oxide after the TPR analyses.

The intensities and peak shapes of the Cu^0 peaks [(111) and (200) reflections at 43.5° and 50.5°, respectively] show that the Cu^0 aggregates are much larger for the unpromoted sample. High-temperature sintering in He increases the sharpness of the Cu^0 XRD peaks and thus the crystallite size. As the results in Figure 5 show, there is an indirect relationship between Cu^0 crystallite size and catalytic activity. This Cu^0 particle-size effect is related to the nature of the Cu^0 sites on the small Cu^0 crystallites and not the number of Cu^0 sites. The small temperature dependency for H_2 chemisorption is more indicative of H_2 chemisorption on group 8 metals such as Rh or Pt, which chemisorb H_2 in a nonactivated manner to form a somewhat hydridic

H species (18). Since hydrides are stronger reducing agents than heterolytically dissociated H_2, typically associated with metal oxides, a lower activation energy for CH_3OH formation is not unexpected for the promoted Cu-Cr oxides.

We conclude, therefore, that in addition to Cu^+, which is required for CO chemisorption, metallic Cu^0 centers are required for facile H_2 chemisorption and subsequent reduction to form CH_3OH over Cu-Cr oxide.

Acknowledgments. We thank Dr. Henry Gysling for providing the $LaRhO_3$ and $GdCoO_3$ samples and for helpful discussions concerning their preparations.

LITERATURE CITED

(1) Ichikawa, M.; Fukushima, T. J. Chem. Soc., Chem. Commun. 1985, 321.
(2) Kawai, M.; Uda, M.; Ichikawa, M. J. Phys. Chem. 1985, 89, 1654.
(3) Wilson, T. P.; Kasai, P. H.; Ellgen, P. C. J. Catal. 1981, 69, 193.
(4) Watson, P. R.; Somorjai, G. A. J. Catal. 1982, 74, 282.
(5) Castner, D. G.; Blackadar, R. L.; Somorjai, G. A. J. Catal. 1980, 66, 257.
(6) Klier, K. Adv. Catal. 1982, 31, 243.
(7) Apai, G.; Monnier, J. R.; Hanrahan, M. J. Appl. Surf. Sci. 1984, 19, 307.
(8) Monnier, J. R.; Hanrahan, M. J.; Apai, G. J. Catal. 1985, 92, 119.
(9) Fleisch, T. H.; Mieville, R. L. J. Catal. 1984, 90, 165.
(10) Okamoto, Y.; Fukino, K.; Imanaka, T.; Teranishi, S. J. Chem. Soc., Chem. Commun. 1982, 1405.
(11) Gallagher, P. K. Mat. Res. Bull. 1968, 3, 225.
(12) Wold, A.; Post, B.; Banks, E. J. Am. Chem. Soc. 1957, 79, 6365.
(13) Carreiro, L.; Qian, Y.-T.; Kershaw, R.; Dwight, K.; Wold, A. Mat. Res. Bull. 1985, 20, 619.
(14) Carreiro, L. Ph.D. Thesis, Brown Univ., 1985.
(15) Gentry, S. J.; Hurst, N. W.; Jones, A. J. Chem. Soc. Trans. Faraday Soc. 1979, 75, 1688.
(16) Orita, H.; Naito, S.; Tamaru, K. J. Catal. 1984, 90, 183.
(17) Solymosi, F.; Erdohelyi, A. Surf. Sci. Lett. 1981, 110, L630.
(18) Bond, G. C. "Catalysis by Metals"; Academic Press: New York, 1962; pp 65-103.

Figure 2. Rh 3d XPS of $LaRhO_3$ as a function of pretreatment.

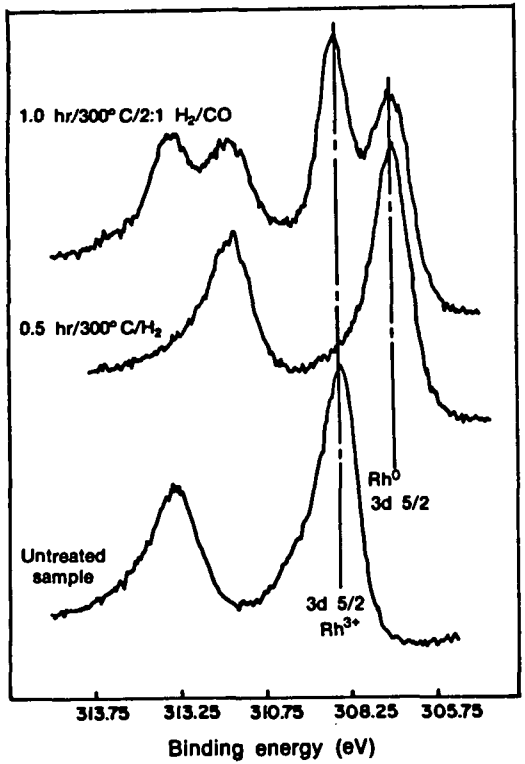

Figure 1. Temperature-programmed reduction in flowing H_2 of $LaRhO_3$ and $GdCoO_3$. Heating rate = 10°C/min. Sample weights: $LaRhO_3$ = 100 mg, $GdCoO_3$ = 350 mg.

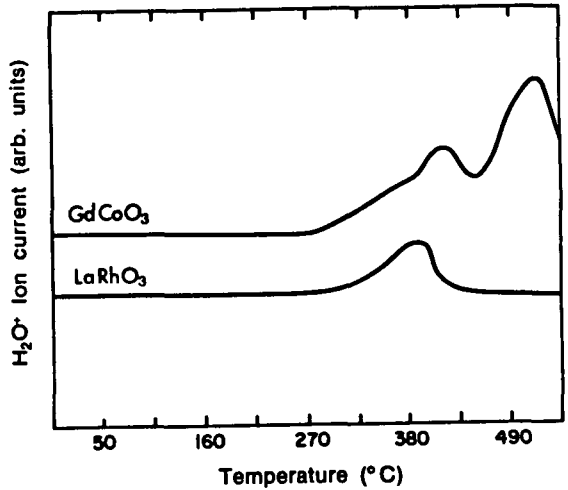

Figure 4. Fischer-Tropsch activity of reduced $GdCoO_3$. Reaction conditions: 250 °C, 800 psig overall pressure, 1:1 H_2/CO; catalysts pretreated for 1 h at 280 °C in 1 atm of flowing H_2.

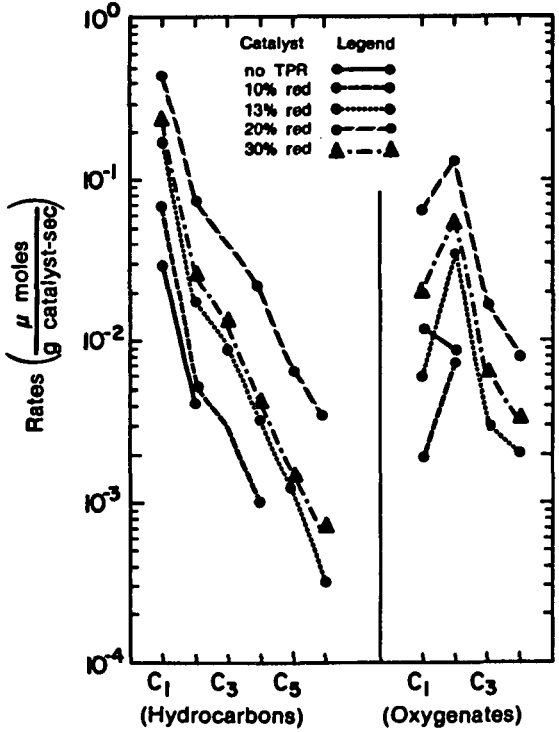

Figure 3. Fischer-Tropsch activity of $LaRhO_3$ as a function of temperature.

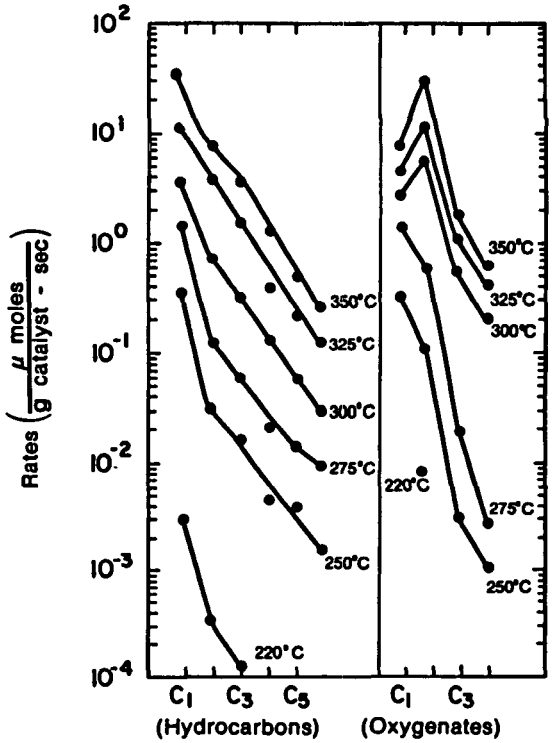
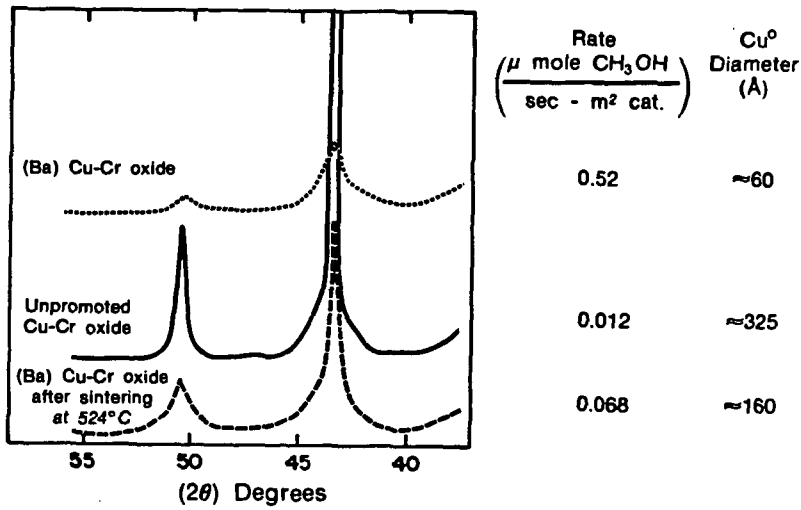
Figure 5. X-ray diffraction patterns after TPR and sintering.